

---

---

# Increased $^{68}\text{Ga}$ -DOTATATE Uptake in PET Imaging Discriminates Meningioma and Tumor-Free Tissue

Walter Rachinger\*<sup>1</sup>, Veit M. Stoecklein\*<sup>1</sup>, Nicole A. Terpolilli<sup>1</sup>, Alexander R. Haug<sup>2,3</sup>, Lorenz Ertl<sup>4</sup>, Julia Pöschl<sup>5</sup>, Ulrich Schüller<sup>5</sup>, Christian Schichor<sup>1</sup>, Niklas Thon<sup>1</sup>, and Jörg-Christian Tonn<sup>1</sup>

<sup>1</sup>Department of Neurosurgery, University of Munich, Munich, Germany; <sup>2</sup>Department of Nuclear Medicine, University of Munich, Munich, Germany; <sup>3</sup>Division of Nuclear Medicine, Department of Biomedical Imaging and Image-Guided Therapy, Medical University Vienna, Vienna, Austria; <sup>4</sup>Department of Neuroradiology, University of Munich, Munich, Germany; and <sup>5</sup>Center for Neuropathology and Prion Research, University of Munich, Munich, Germany

---

Meningiomas are known to express somatostatin receptor 2 (SSTR2). PET using the SSTR2 analog  $^{68}\text{Ga}$ -DOTATATE has recently been introduced for imaging of meningiomas. However, a systematic correlation between  $^{68}\text{Ga}$ -DOTATATE uptake, SSTR2 expression, and histology (including tumor-free scar tissue) is still lacking. For elucidation, we conducted this prospective study.

**Methods:** Twenty-one adult patients with primary ( $n = 12$ ) or recurrent ( $n = 9$ ) meningiomas were prospectively enrolled. Preoperative MR imaging and  $^{68}\text{Ga}$ -DOTATATE PET scans were fused and used for a spatially precise neuronavigated tissue-sampling procedure during tumor resection. Histopathologic diagnosis included immunohistochemical determination of SSTR2 expression. At each individual sampling site, the maximum standardized uptake value ( $\text{SUV}_{\text{max}}$ ) of  $^{68}\text{Ga}$ -DOTATATE was correlated with MR imaging findings, histology, and semiquantitative SSTR2 expression. **Results:** One hundred fifteen samples (81 tumor, 34 tumor-free) were obtained. There was a significant positive correlation between  $\text{SUV}_{\text{max}}$  and SSTR2 expression. Receiver-operating characteristic analysis revealed a threshold of 2.3 for  $\text{SUV}_{\text{max}}$  to discriminate between tumor and non-tumoral tissue. Regarding the detection of tumor tissue, PET imaging showed a higher sensitivity (90% vs. 79%;  $P = 0.049$ ), with specificity and positive predictive values similar to MR imaging, for both de novo and recurrent tumors. **Conclusion:**  $^{68}\text{Ga}$ -DOTATATE uptake correlates with SSTR2 expression and offers high diagnostic accuracy to delineate meningioma from tumor-free tissue even in recurrent tumors after previous therapy. Our findings substantiate an important role for  $^{68}\text{Ga}$ -DOTATATE PET in meningioma management.

**Key Words:** DOTATATE; imaging; meningioma; neuronavigation; PET; somatostatin receptor

**J Nucl Med 2015; 56:347–353**

DOI: 10.2967/jnumed.114.149120

---

**M**eningiomas represent 20% of all intracranial tumors with a female-to-male ratio of 3:2 (1). They express a variety of receptors including somatostatin receptor subtype 2 (SSTR2) (2).

Received Oct. 8, 2014; revision accepted Dec. 26, 2014.

For correspondence or reprints contact: Walter Rachinger, Department of Neurosurgery, University of Munich, Marchioninistrasse 15, 81377 Munich, Germany.

E-mail: walter.rachinger@med.uni-muenchen.de

\*Contributed equally to this work.

Published online Jan. 29, 2015.

COPYRIGHT © 2015 by the Society of Nuclear Medicine and Molecular Imaging, Inc.

The mainstay of therapy is microsurgery, radiosurgery, fractionated radiation therapy, or any combination thereof (3–5). For target volume definition concerning any of these treatment modalities, MR imaging is the gold standard. However, in infiltrative lesions and in the case of scar formation after surgery or radiation, MR imaging might be limited in terms of sensitivity and specificity of diagnosis due to, for example, unspecific contrast enhancement of scar tissue.

Because of high levels of expression of SSTR2 in meningiomas and an excellent tumor-to-background ratio, imaging with somatostatin receptor ligands has been established as a method for the detection and target volume definition of meningiomas before radiotherapy (6,7). In recent years, somatostatin receptor scintigraphy has been increasingly replaced by PET/CT because of the significantly improved spatial resolution of PET/CT and the ability to quantify biodistribution (8). The somatostatin analogs DOTATOC or DOTATATE have shown a high affinity for SSTR2 (9). Labeled with the positron-emitting generator nuclide  $^{68}\text{Ga}$ , DOTATATE is increasingly used for PET investigation of meningiomas, particularly for treatment planning (10–12).

A systematic correlative analysis between histopathology, expression of SSTR2, and uptake of  $^{68}\text{Ga}$ -DOTATATE, however, is still lacking. For elucidation, we conducted this prospective study. Special focus was set on the diagnostic accuracy of  $^{68}\text{Ga}$ -DOTATATE PET as compared with MR imaging in the de novo situation and at tumor recurrence after therapy.

## MATERIALS AND METHODS

### Patients

In our department,  $^{68}\text{Ga}$ -DOTATATE PET/CT is routinely performed in patients with suspected meningioma in complex locations (Fig. 1). For this study, adult patients with either falx/parasagittal or skull-base tumors suspected as de novo or recurrent meningioma were prospectively assigned to standardized MR imaging and  $^{68}\text{Ga}$ -DOTATATE PET/CT before neuronavigated microsurgical resection. Approval was obtained from the local institutional review board (AZ 216/04). All enrolled patients gave informed consent.

### MR Imaging

Standardized MR imaging investigation was performed on 1.5- or 3.0-T scanners (Magnetom Symphony [Siemens] or Signa HDxt [GE Healthcare]) directly before surgery. The imaging protocol consisted of diffusion-weighted imaging, contrast-enhanced MR angiography, axial T2-weighted sequences (slice thickness, 2 mm), and 3-dimensional T1-weighted sequences (fast spoiled gradient-echo; slice thickness, 1 mm; field of view, 220 mm; matrix, 256 × 256; spatial resolution, 0.85 mm

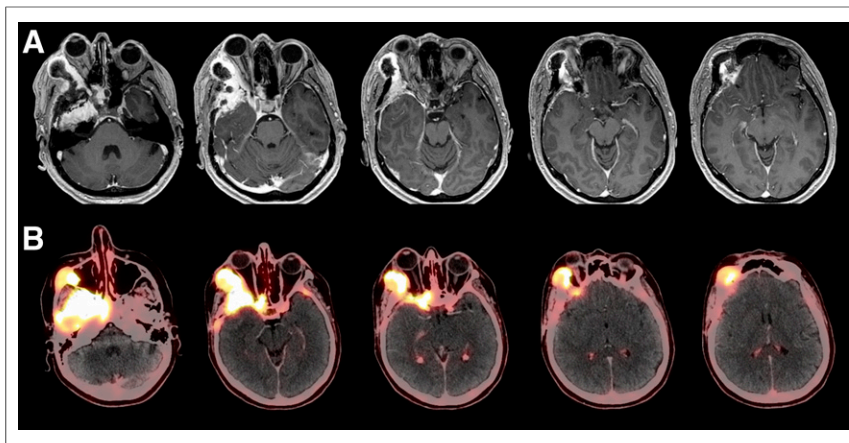


**FIGURE 1.** (A) MR imaging scan of 44-y-old male patient with recurrent sphenoorbital meningioma with previous surgery in 2005. (B) Corresponding fused PET/CT scan ( $128 \times 128$  pixels) shows extensive infiltration of osseous skull base by meningioma.

isovoxel in plane) before and after administration of intravenous contrast agent (0.1 mmol/kg of body weight of gadobenate dimeglumine [Multihance; Bracco Imaging S.p.A.]).

#### **<sup>68</sup>Ga-DOTATATE PET Image Acquisition and Analysis**

<sup>68</sup>Ga-DOTATATE PET scans were acquired within a maximum of 45 d before surgery. At the time of PET investigation, no patient was treated with steroids. PET data acquisition was performed with a PET/CT scanner (Biograph 64; Siemens Medical Solutions). Sixty minutes after intravenous injection of 150 MBq of <sup>68</sup>Ga-DOTATATE, the combined examination commenced with a topogram to define the PET/CT examination range (2 bed positions to cover the whole cranium including the craniocervical junction). Unenhanced CT scans were obtained first for attenuation correction of PET data and for anatomic correlation. Subsequently, the PET scan was done by acquiring static emission data for 4 min per bed position. PET images were reconstructed using an iterative algorithm (ordered-subset expectation maximization: 4 iterations, 8 subsets). Unenhanced CT data were reconstructed with a slice thickness of 5 mm (axial) and an increment of 5 mm. The reconstructed PET, CT, and fused images were displayed on the manufacturer's workstation (e-soft; Siemens Medical Solutions) in axial, coronal, and sagittal planes, with a resolution of  $128 \times 128$  pixels for the PET and  $512 \times 512$  pixels for the CT images.

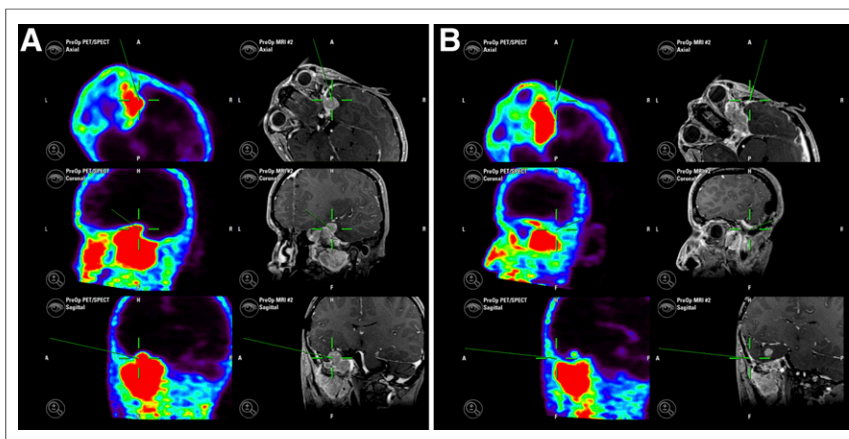


**FIGURE 2.** Intraoperative screenshots obtained during sampling of tumor tissue (A) and dura (B). PET ( $128 \times 128$  pixels) and MR imaging data are simultaneously displayed and were used to guide sampling process.

Because of the high energy of the <sup>68</sup>Ga positrons, the actual spatial resolution of reconstructed PET images was estimated to be in the range of 8–10 mm.

#### **<sup>68</sup>Ga-DOTATATE PET-Guided Resection and Tissue-Sampling Procedure**

MR imaging and <sup>68</sup>Ga-DOTATATE PET data were coregistered (iPlan 2.6 cranial; BrainLAB) with data from intraoperative CT (iCT-Suite [Siemens]); unenhanced scans; slice thickness, 1 mm) and used for 3-dimensional tumor visualization during surgery (Fig. 2). iCT was used for referencing because of its superior accuracy (0.5 mm) (13–15). Additionally, iCT offered the opportunity to assess the extent of resection during surgery. Intraoperative neuronavigation was used for spatially precise tissue sampling during maximal safe resection. Tissue samples were categorized as tumoral or nontumoral tissues (peritumoral dura, bone, or scar) according to the intraoperative impression. The biopsy site was accurately indicated by the registration pointer (median accuracy, 1 mm) and documented by a screenshot of the respective axial, coronal, and sagittal planes of both coregistered MR images and <sup>68</sup>Ga-DOTATATE PET images. Tissue samples were paraffin-embedded for further analyses.

#### **Analysis of PET and MR Imaging at Biopsy Sites**

Interpretation of MR images at each individual point of tissue sampling was performed by an experienced neuroradiologist who was masked to the results of PET scans, the surgeons' intraoperative findings, and definitive histology. Radiologic diagnosis of active tumor tissue was made at the discretion of and based on the experience of the neuroradiologist. MR imaging-based criteria for tumor tissue were contrast enhancement on T1-weighted sequences and its anatomic correlation to the T2-weighted images.

Results from PET analyses were evaluated by an experienced physician for nuclear medicine who was masked to all other study findings. A region of interest was defined for each biopsy site as indicated by PET-based neuronavigation. Maximum standardized uptake values ( $SUV_{max}$ ) of <sup>68</sup>Ga-DOTATATE were calculated for these regions by determining the maximum PET tracer uptake and correlating it with the injected dose and patient body weight: [ $SUV_{max} = \text{maximum activity concentration}/(\text{injected dose}/\text{body weight})$ ].

#### **Histopathology and Immunostaining**

All tumors were fixed in 4% neutral formalin for 24 h at room temperature, embedded in paraffin, and cut into consecutive 4- $\mu$ m-thick sections. Histopathologic diagnosis of meningioma was done according to the current World Health Organization (WHO) classification of tumors of the central nervous system (16). For the subsequent immunohistochemistry, sections were deparaffinized and subjected to standardized staining on a benchmark staining machine with a 3, 3'-diaminobenzidine detection system according to the manufacturer's instructions (Ventana Medical Systems). A commercially available primary antibody against SSTR2 (rabbit antihuman, clone SS-800;

Gramsch Laboratories) was used at a dilution of 1:1,000. Nuclear counterstaining was performed using Mayer hemalaun. The specificity of the binding was assessed by omitting the primary antiserum or replacing it with normal rabbit serum or phosphate-buffered saline solution (pH 7.4). Moreover, human samples of pituitary gland tissue were used as a positive control for the SSTR2 immunoreaction.

Semiquantitative analysis was performed in an independent and masked fashion by 2 experienced board-certified neuropathologists. To enable a comparability with the literature (17,18), SSTR2 expression was classified according to a 4-scaled staining score as follows: positive immunostaining of 0%–25%, 26%–50%, 51%–75%, and 76%–100% of the respective tissue translated to a corresponding staining score of grade 1 (no/weak), grade 2 (mild/modest), grade 3 (moderate), and grade 4 (strong). In cases for which the scoring of tissue samples was discordant between the 2 neuropathologists, the senior neuropathologist cast the tie-breaking vote.

### Statistical Analysis

The distribution of variables between subgroups was analyzed by  $\chi^2$  statistics (for dichotomized variables) and the Wilcoxon test (for continuously scaled variables). *P* values of 0.05 or less were considered statistically significant. A statistical software package (SPSS Statistics 19; IBM) was used for these tests.

## RESULTS

### Patient Characteristics

Between October 2010 and October 2013, 21 patients (8 men, 13 women) were enrolled. Patient and tumor characteristics are presented in Table 1. Nine (43%) patients experienced recurrent

disease and had undergone 1 (*n* = 4) or more surgeries (*n* = 5) plus Cyberknife (Accuray Inc.) radiosurgery (*n* = 2) before study inclusion. One patient had been treated with conventional radiotherapy for childhood acute lymphatic leukemia.

Tumor locations were the sphenoid wing or sphenoorbital in 11 (42%) patients, the olfactory groove in 1 (5%), falcine or parasagittal in 6 (29%), and the convexity in 3 (14%). A meningioma was histologically verified in all cases. Further classification revealed a transitional meningioma (WHO grade I) in 7 (33%) patients and meningotheliomatous or secretory meningioma (both WHO grade I) in 3 (14%) patients each. In another 3 (14%) patients, grade I meningiomas were not further classified. An atypical meningioma WHO grade II was found in 4 (19%) patients and an anaplastic meningioma WHO grade III in 1 (5%) patient.

The date of last follow-up was March 31, 2014. The median follow-up was 12 mo (range, 3–39 mo). During the follow-up period, 5 patients experienced a tumor recurrence. Two of these patients underwent resurgery. Three patients underwent radiotherapy after primary surgery.

### Correlative Analyses

Overall, 115 biopsies were collected (median, 5/patient; range, 1–13). A detailed correlation of histology,  $SUV_{max}$ , MR imaging findings, and SSTR2 expression for each individual biopsy is presented in Supplemental Table 1 (supplemental materials are available at <http://jnm.snmjournals.org>). Because the level of SSTR2 expression was found to be heterogeneous in 16 of 21 patients, we used a samplewise approach to analyze our data that would yield more information, especially with regard to the spatial resolution within the tumor.

**TABLE 1**  
Patient and Tumor Characteristics

Patient no.	Age (y)	Sex	Histology	Tumor location	De novo/ recurrent	Previous radiation	No. of samples
1	43	F	Meningotheliomatous WHO I	Convexity	0	0	4
2	48	F	Transitional WHO I	Sphenoorbital	0	0	4
3	57	F	Secretory WHO I	Sphenoid wing	0	0	7
4	46	M	Meningotheliomatous WHO I	Falx	1 (1×)	0	13
5	54	F	Transitional WHO I	Sphenoorbital	0	0	3
6	55	F	Transitional WHO I	Convexity	0	0	4
7	44	M	Transitional WHO I	Sphenoorbital	1 (3×)	0	3
8	40	F	Secretory WHO I	Sphenoid wing	0	0	2
9	52	F	WHO I	Sphenoorbital	1 (2×)	0	7
10	48	F	Transitional WHO I	Sphenoid wing	0	0	2
11	49	F	WHO I	Sphenoorbital	0	0	2
12	60	M	Atypical WHO II	Falx	1 (1×)	2 Cyberknife	8
13	65	F	Transitional WHO I	Olfactory groove	0	0	1
14	44	F	WHO I	Sphenoorbital	1(4×)	0	10
15	67	M	Atypical WHO II	Falx	1 (3×)	0	8
16	51	M	Anaplastic WHO III	Convexity	1 (1×)	2 Cyberknife	6
17	65	F	Meningotheliomatous WHO I	Parasagittal	0	0	6
18	61	M	Atypical WHO II	Parasagittal	1 (1×)	0	6
19	51	M	Transitional WHO I	Falx	0	0	5
20	48	F	Secretory WHO I	Sphenoorbital	0	0	9
21	29	M	Atypical WHO II	Sphenoid wing	1 (2×)	1 Conventional radiotherapy	5

Histologic evaluation of each individual biopsy revealed tumor tissue in 81 (70.4%) samples. Thirty-eight (47.0%) samples originated from de novo and 43 (53.0%) from recurrent tumors. A WHO grade I meningioma was found in 59 (72.8%) specimens and a grade II or III meningioma in 17 (14.8%) and 5 (4.3%) specimens, respectively. Thirty-four (29.6%) specimens were tumor-free (15 scar, 14 normal dura, 5 bone). Ten of these samples were harvested from 5 patients with de novo (6 normal dura, 4 bone) and the remaining 24 samples from 7 patients with recurrent meningiomas (15 scar, 8 normal dura, 1 bone).

### MR Imaging

According to MR imaging interpretation, tumor tissue was suspected in 76 (39 tumor-free) of 115 biopsies. Radiologic classification matched histologic diagnoses in 86 of 115 (74.8%) samples. Overall, MR imaging differentiated tumor from tumor-free tissue with a 79.0% sensitivity and 64.7% specificity. The positive predictive value for MR imaging was 84.2%. The respective values did not differ for the subgroups of de novo and recurrent tumors.

### <sup>68</sup>Ga-DOTATATE PET

PET analyses considering all biopsy samples revealed a median SUV<sub>max</sub> of 6.6 (range, 0.1–106.6). A significant correlation between SUV<sub>max</sub> and histologic diagnosis was seen: <sup>68</sup>Ga-DOTATATE uptake clearly differed in tumor and tumor-free tissue (median SUV<sub>max</sub>, 10.1 vs. 1.2; *P* < 0.001). No difference was seen between <sup>68</sup>Ga-DOTATATE uptake in de novo and recurrent (median SUV<sub>max</sub>, 12.8 vs. 9.8) or in grade I and grade II/III (median SUV<sub>max</sub>, 9.9 vs. 10.3) meningioma tissue (*P* = 0.154, *P* = 0.433).

Receiver-operating-characteristic (ROC) curve analysis revealed best differentiation between tumor and tumor-free tissues at an SUV<sub>max</sub> threshold of 2.3 (number of samples with an SUV<sub>max</sub> < 2.3 was 33, and ≥2.3 it was 82): overall, sensitivity, specificity, and positive predictive values for PET to detect vital tumor tissue were 90.1%, 73.5%, and 89.0%, respectively.

Results from PET and MR imaging investigations were congruent in 72 of 81 (88.9%) tumor samples and in 29 of 34 (85.3%) tumor-free samples. The sensitivity to detect tumor tissue was higher for PET than MR imaging (90.1% vs. 79.0%, *P* = 0.049); this was the case in both de novo (92.3% vs. 79.5%, *P* = 0.039) and recurrent tumors (88.1% vs. 76.7%, *P* = 0.045). The respective specificities and positive predictive values did not differ. Contingency tables for all samples are shown in Tables 2 and 3, for samples from de novo tumors in Tables 4 and 5, and for samples from recurrent tumors in Tables 6 and 7. Sensitivity,

**TABLE 2**  
Contingency Table for <sup>68</sup>Ga-DOTATATE PET and All Samples

	PET	Tumor	No tumor	Total
Positive (SUV <sub>max</sub> > 2.3)		73	9	82
Negative (SUV <sub>max</sub> < 2.3)		8	25	33
Total		81	34	115

Sensitivity, 90.1%; specificity, 73.5%; positive predictive value, 89.0%.

**TABLE 3**  
Contingency Table for MR Imaging and All Samples

MR imaging	Tumor	No tumor	Total
Positive	64	12	76
Negative	17	22	39
Total	81	34	115

Sensitivity, 79.0%; specificity, 64.7%; positive predictive value, 84.2%.

specificity, and positive predictive values for PET and MR imaging in these groups are also shown.

PET identified 9 additional, distant lesions as being suggestive of meningioma; these lesions were also noted on MR imaging in 5 cases after re-review of the scans.

### SSTR2 Expression

The expression of SSTR2 was classified as grade 1 in 42 samples, grade 2 in 16, grade 3 in 27, and grade 4 in 30, respectively. No difference was found between tumor samples harvested at first diagnosis and those from recurrent disease. Increased SSTR2 expression (≥grade 2) was significantly associated with tumor tissue (*P* < 0.001). Figure 3 shows a negative sample (dura) and a representative example of grade 4 immunostaining. However, tumor specimens of 3 de novo and 6 recurrent meningiomas (all WHO grade I) displayed no or only weak SSTR2 staining (grade 1).

There was a positive correlation between categoric SSTR2 expression and dichotomized SUV<sub>max</sub> (*P* = 0.008). At least SSTR2 expression grade 2 was seen in 65 (89.0%) of 73 biopsy samples exhibiting an SUV<sub>max</sub> of 2.3 or greater. No or only weak (grade 1) SSTR2 expression was noted in 24 (57.1%) of 42 biopsies exhibiting an SUV<sub>max</sub> of less than 2.3. In 15 samples, SSTR2 staining and SUV<sub>max</sub> were discordant: 9 samples stained only weakly for SSTR2 (grade 1) despite an SUV<sub>max</sub> of 2.3 or greater. Seven of these samples were tumor-free (4 dura, 3 scar tissue), whereas tumor was found in 2 of these samples. In 6 samples, moderate or strong (grade 3 or 4) SSTR2 staining was demonstrated, but SUV<sub>max</sub> was low (<2.3). All of these samples contained tumor tissue.

### DISCUSSION

Meningioma recurrence after surgical resection occurs in up to 20% of cases, even if the tumor was considered histologically

**TABLE 4**  
Contingency Table for <sup>68</sup>Ga-DOTATATE PET and Samples from De Novo Tumors

	PET	Tumor	No tumor	Total
Positive (SUV <sub>max</sub> > 2.3)		36	3	39
Negative (SUV <sub>max</sub> < 2.3)		3	7	10
Total		39	10	49

Sensitivity, 92.3%; specificity, 70.0%; positive predictive value, 92.3%.

**TABLE 5**

Contingency Table for MR Imaging and Samples from De Novo Tumors

MR imaging	Tumor	No tumor	Total
Positive	31	4	35
Negative	8	6	14
Total	39	10	49

Sensitivity, 79.5%; specificity, 60.0%; positive predictive value, 88.6%.

benign (WHO grade I) (19). Recurrence rates are substantially higher if only subtotal surgical removal could be achieved; in these cases a course of adjuvant radiation therapy to lower probability of recurrence or, alternatively, close imaging follow-up to pick up recurrence early should be considered (20). An ideal imaging modality to guide meningioma management should therefore be as accurate as possible to delineate tumor from tumor-free tissue in order to achieve the maximal safe resection and to detect remaining or recurrent tumor tissue as reliably as possible. Contrast-enhanced MR imaging (ceMRI) is currently the imaging modality of choice for both diagnostic evaluation and treatment planning. However, the diagnostic accuracy of MR imaging is often considered as limited, especially in complex anatomic situations in which bone infiltration or scar tissue is present. Additional imaging modalities to detect tumor remnants or recurrence more precisely are therefore needed.

In recent years, molecular imaging has gained increasing importance in diagnosing intracranial neoplasms and, ultimately, in guiding treatment of these diseases (21). Among the available imaging modalities, PET with  $^{68}\text{Ga}$ -DOTATATE as a tracer has been used for imaging of meningiomas. The molecular target of  $^{68}\text{Ga}$ -DOTATATE is the surface receptor SSTR2, which has been suggested to be constitutively expressed by all meningiomas (9).

This is the first study, to our knowledge, that systematically validates  $^{68}\text{Ga}$ -DOTATATE imaging of meningiomas by performing a spatially precise correlative analysis of PET imaging, histopathology, and SSTR2 expression. The applied iCT-based fusion protocol of MR imaging and PET data for 3-dimensional neuro-navigated biopsy sampling in combination with the post hoc masked analysis of  $\text{SUV}_{\text{max}}$  (PET)/contrast enhancement (MR imaging) for each individual site of biopsy offers a high spatial accuracy. Using this approach, we were able to show that  $^{68}\text{Ga}$ -DOTATATE PET indeed offers a high sensitivity for the detection

**TABLE 6**Contingency Table for  $^{68}\text{Ga}$ -DOTATATE PET and Samples from Recurrent Tumors

PET	Tumor	No tumor	Total
Positive ( $\text{SUV}_{\text{max}} > 2.3$ )	37	6	43
Negative ( $\text{SUV}_{\text{max}} < 2.3$ )	5	18	23
Total	42	24	66

Sensitivity, 88.1%; specificity, 75.0%; positive predictive value, 86.0%.

**TABLE 7**

Contingency Table for MR Imaging and Samples from Recurrent Tumors

MR imaging	Tumor	No tumor	Total
Positive	33	8	41
Negative	9	16	25
Total	42	24	66

Sensitivity, 78.6%; specificity, 66.7%; positive predictive value, 80.5%.

of vital meningioma tissue (90.1%). Moreover, a strong correlation between  $\text{SUV}_{\text{max}}$  and semiquantitative SSTR2 expression was confirmed, supporting the diagnostic validity of  $^{68}\text{Ga}$ -DOTATATE PET. No difference was seen between de novo and recurrent tumors with respect to both median  $\text{SUV}_{\text{max}}$  and SSTR2 expression pattern, indicating that SSTR2 is constitutively expressed in meningiomas throughout the course of disease. However, 9 of our samples with histologically proven tumor tissue showed no or only weak SSTR2 expression, which is discordant with the aforementioned report (2) and might explain false-negative results in  $^{68}\text{Ga}$ -DOTATATE PET for meningiomas. Accordingly,  $\text{SUV}_{\text{max}}$  was low in these samples.

Our study did not reveal a correlation between  $\text{SUV}_{\text{max}}$  and WHO grade, indicating that SSTR2 expression is independent of the differentiation status of meningioma cells. In contrast, certain histologic meningioma subtypes were associated with increased  $\text{SUV}_{\text{max}}$ . Secretory meningioma showed the highest  $\text{SUV}_{\text{max}}$ , which is in line with data of a histopathologic study that did not find a correlation between tumor grade and expression of SSTR2 but between histologic subtype and SSTR2 (22). Thus,  $^{68}\text{Ga}$ -DOTATATE PET accurately depicts SSTR2 expression but does not discriminate different WHO grades in meningiomas.

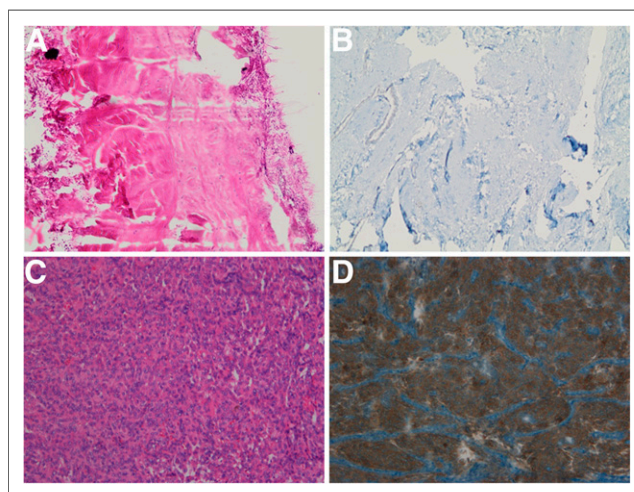


**FIGURE 3.** Immunostaining for SSTR2 and corresponding hematoxylin and eosin stains. (A) Hematoxylin and eosin stain of dura. (B) SSTR2 stain of same sample as in A is negative. (C) Hematoxylin and eosin stain of meningioma tissue. (D) More than 75% of cells of same sample as in C were positive for SSTR2 (brown color). This sample was therefore classified as grade 4 SSTR2 expression (strong expression).

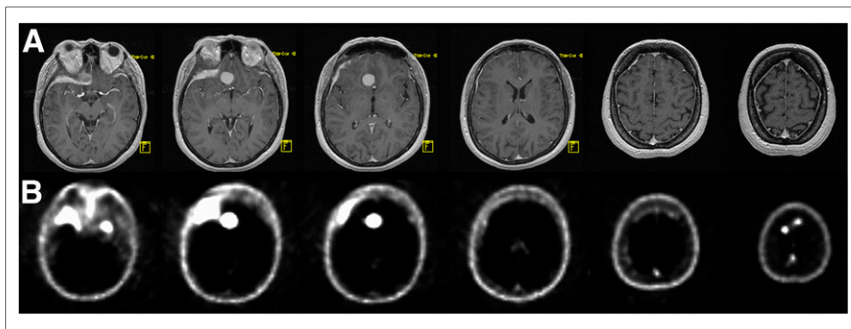


**FIGURE 4.** MR imaging (A) and corresponding  $^{68}\text{Ga}$ -DOTATATE PET (B) scans ( $128 \times 128$  pixels) of 48-y-old female patient with sphenoorbital meningioma. PET scan shows additional parafalcine tumor manifestations that are not visible on MR imaging scan.

ROC analysis revealed the threshold for best discrimination of tumor and tumor-free tissue at an  $\text{SUV}_{\text{max}}$  of 2.3. Best discrimination of tumor and tumor-free tissue was found at an  $\text{SUV}_{\text{max}}$  of 2.3: at this cutoff, tumor tissue was identified with a high sensitivity ( $\sim 90\%$ ) without risking overtreatment due to unreasonably low specificity, which is desirable in an imaging modality used for treatment decision making. Because the ROC analysis in our study was based on actual histopathologic diagnoses, this value might serve as guidance for further studies using  $^{68}\text{Ga}$ -DOTATATE PET in meningioma diagnosis and therapy.

It is a common perception that scar tissue is difficult to separate from tumor tissue on ceMRI. We hypothesized that  $^{68}\text{Ga}$ -DOTATATE PET might provide higher diagnostic accuracy regarding the detection of vital tumor tissue in this situation. Indeed, our findings showed statistically significant higher sensitivity for  $^{68}\text{Ga}$ -DOTATATE PET in patients with recurrent tumors than for ceMRI.  $^{68}\text{Ga}$ -DOTATATE PET proved also to be more sensitive than ceMRI in delineating untreated meningioma tissue. As shown in Figure 4, the increased sensitivity of  $^{68}\text{Ga}$ -DOTATATE PET led to the detection of additional, so far undiagnosed meningiomas in 9 patients, which is in line with a recent study that compared  $^{68}\text{Ga}$ -DOTATATE PET and ceMRI with regard to the detection of meningiomas (10). However, this particular study lacked histopathologic confirmation of PET findings.

The specificity of  $^{68}\text{Ga}$ -DOTATATE PET was similar but not better than ceMRI. The significance of this finding, however, is critically limited by the low number of tumor-negative samples in our study, as samples clearly taken from tumor-free areas were kept to the bare minimum for safety reasons. The combination of a superior sensitivity with a noninferior specificity proved that  $^{68}\text{Ga}$ -DOTATATE PET provides additional useful information that might help to overcome critical limitations of solely MR imaging-based assessment of suspected tumor recurrence. In a recent study comparing PET/CT with a PET/MR imaging hybrid system, the latter was reported to deliver even better spatial resolution (23). In our study, we overcame this limitation by fusing PET/CT with MR imaging using the navigation software.

Altogether, our data support and justify the use of  $^{68}\text{Ga}$ -DOTATATE PET for refined planning of local therapies such as resection, radiotherapy, or peptide receptor therapy, which is currently entering clinical practice (24). In our opinion, the improved sensitivity offered by  $^{68}\text{Ga}$ -DOTATATE PET to detect vital meningioma tissue is of great clinical utility. Its superior sensitivity will help to identify the true extent of tumor infiltration, especially in recurrent tumors being intermingled with scar tissue. DOTATATE

PET-guided planning of surgical resection and radiotherapy might therefore avoid undertreatment. Whether this could help to decrease the likelihood of recurrence has to be evaluated in forthcoming prospective studies. Furthermore, using  $^{68}\text{Ga}$ -DOTATATE PET for follow-up in high-risk patients allows for early detection of recurring disease and corresponding aggressive early treatment.

## CONCLUSION

We present the first study, to our knowledge, that correlates  $^{68}\text{Ga}$ -DOTATATE PET, MR imaging findings, tumor histology, and SSTR2 expression, thereby providing histologic validation of this molecular imaging modality. ROC analysis revealed the threshold for best discrimination of tumor and tumor-free tissue at an  $\text{SUV}_{\text{max}}$  of 2.3.  $^{68}\text{Ga}$ -DOTATATE PET had a higher sensitivity than ceMRI for the detection of active tumor tissue in both untreated and recurrent meningioma. These findings substantiate an important role for  $^{68}\text{Ga}$ -DOTATATE PET in therapy planning by delineating resection margins and target volumes for radiation therapy of tumors that are in complex locations or recurrent.

## DISCLOSURE

The costs of publication of this article were defrayed in part by the payment of page charges. Therefore, and solely to indicate this fact, this article is hereby marked "advertisement" in accordance with 18 USC section 1734. No potential conflict of interest relevant to this article was reported.

## REFERENCES

- Dolecek TA, Propp JM, Stroup NE, Kruchko C. CBTRUS statistical report: primary brain and central nervous system tumors diagnosed in the United States in 2005-2009. *Neuro-oncol.* 2012;14(suppl 5):v1-v49.
- Dutour A, Kumar U, Panetta R, et al. Expression of somatostatin receptor subtypes in human brain tumors. *Int J Cancer.* 1998;76:620-627.
- Westphal M, Lamszus K, Tonn J. Meningiomas and meningeal tumors. In: Tonn J, Westphal M, Rutka J, eds. *Oncology of CNS Tumors*. 2nd ed. New York, NY: Springer; 2010:95-118.
- Combs SE, Ganswindt U, Foote RL, Kondziolka D, Tonn JC. State-of-the-art treatment alternatives for base of skull meningiomas: complementing and controversial indications for neurosurgery, stereotactic and robotic based radiosurgery or modern fractionated radiation techniques. *Radiat Oncol.* 2012; 7:226.
- Pechlivanis I, Wawrzyniak S, Engelhardt M, Schmieder K. Evidence level in the treatment of meningioma with focus on the comparison between surgery versus radiotherapy: a review. *J Neurosurg Sci.* 2011;55:319-328.
- Henze M, Dimitrakopoulou-Strauss A, Milker-Zabel S, et al. Characterization of  $^{68}\text{Ga}$ -DOTA-D-Phe1-Tyr3-octreotide kinetics in patients with meningiomas. *J Nucl Med.* 2005;46:763-769.
- Gehler B, Paulsen F, Oksuz MO, et al.  $^{68}\text{Ga}$ -DOTATATE-PET/CT for meningioma IMRT treatment planning. *Radiat Oncol.* 2009;4:56.
- Gabriel M, Decristoforo C, Kendler D, et al.  $^{68}\text{Ga}$ -DOTA-Tyr3-octreotide PET in neuroendocrine tumors: comparison with somatostatin receptor scintigraphy and CT. *J Nucl Med.* 2007;48:508-518.
- Reubi JC, Schar JC, Waser B, et al. Affinity profiles for human somatostatin receptor subtypes SST1-SST5 of somatostatin radiotracers selected for scintigraphic and radiotherapeutic use. *Eur J Nucl Med.* 2000;27:273-282.
- Afshar-Oromieh A, Giesel FL, Linhart HG, et al. Detection of cranial meningiomas: comparison of  $^{68}\text{Ga}$ -DOTATATE PET/CT and contrast-enhanced MRI. *Eur J Nucl Med Mol Imaging.* 2012;39:1409-1415.
- Milker-Zabel S, Zabel-du Bois A, Henze M, et al. Improved target volume definition for fractionated stereotactic radiotherapy in patients with intracranial

- meningiomas by correlation of CT, MRI, and [<sup>68</sup>Ga]-DOTATOC-PET. *Int J Radiat Oncol Biol Phys*. 2006;65:222–227.
12. Henze M, Schuhmacher J, Hipp P, et al. PET imaging of somatostatin receptors using [68Ga]DOTA-d-Phe1-Tyr3-octreotide: first results in patients with meningiomas. *J Nucl Med*. 2001;42:1053–1056.
  13. Uhl E, Zausinger S, Morhard D, et al. Intraoperative computed tomography with integrated navigation system in a multidisciplinary operating suite. *Neurosurgery*. 2009;64:231–239.
  14. Stelter K, Ledderose G, Hempel JM, et al. Image guided navigation by intraoperative CT scan for cochlear implantation. *Comput Aided Surg*. 2012;17:153–160.
  15. Eggers G, Kress B, Rohde S, Muhling J. Intraoperative computed tomography and automated registration for image-guided cranial surgery. *Dentomaxillofac Radiol*. 2009;38:28–33.
  16. Louis DN, Ohgaki H, Wiestler OD, et al. The 2007 WHO classification of tumours of the central nervous system. *Acta Neuropathol*. 2007;114:97–109.
  17. Qiu CZ, Wang C, Huang ZX, Zhu SZ, Wu YY, Qiu LL. Relationship between somatostatin receptor subtype expression and clinicopathology, Ki-67, Bcl-2 and p53 in colorectal cancer. *World J Gastroenterol*. 2006;12:2011–2015.
  18. Barresi V, Alafaci C, Salpietro F, Tuccari G. Sstr2A immunohistochemical expression in human meningiomas: is there a correlation with the histological grade, proliferation or microvessel density? *Oncol Rep*. 2008;20:485–492.
  19. Maillo A, Orfao A, Sayagués JM, et al. New classification scheme for the prognostic stratification of meningioma on the basis of chromosome 14 abnormalities, patient age, and tumor histopathology. *J Clin Oncol*. 2003;21:3285–3295.
  20. Kaley T, Barani I, Chamberlain M, et al. Historical benchmarks for medical therapy trials in surgery- and radiation-refractory meningioma: a RANO review. *Neuro-oncol*. 2014;16:829–840.
  21. la Fougère C, Suchorska B, Bartenstein P, Kreth F-W, Tonn J-C. Molecular imaging of gliomas with PET: opportunities and limitations. *Neuro-oncol*. 2011;13:806–819.
  22. Durand A, Champier J, Jouvet A, et al. Expression of c-Myc, neurofibromatosis Type 2, somatostatin receptor 2 and erb-B2 in human meningiomas: relation to grades or histotypes. *Clin Neuropathol*. 2008;27:334–345.
  23. Afshar-Oromieh A, Wolf MB, Kratochwil C, et al. Comparison of <sup>68</sup>Ga-DOTATOC-PET/CT and PET/MRI hybrid systems in patients with cranial meningioma: initial results. *Neuro-oncol*. 2014;17:312–319.
  24. Thorwarth D, Henke G, Muller AC, et al. Simultaneous <sup>68</sup>Ga-DOTATOC-PET/MRI for IMRT treatment planning for meningioma: first experience. *Int J Radiat Oncol Biol Phys*. 2011;81:277–283.